Full-Wave Design and Optimization of Circular Waveguide Polarizers With Elliptical Irises

Giorgio Bertin, *Member, IEEE*, Bruno Piovano, *Associate Member, IEEE*, Luciano Accatino, *Member, IEEE*, and Mauro Mongiardo, *Senior Member, IEEE*

***Abstract*—We describe the design and optimization of a new polarizer structure realized in circular waveguide with insertion of elliptical irises. The device is compact, showing a considerable reduction in size and weight when compared to previously known realizations. It requires manufacturing by milling techniques only and, since it is composed entirely by waveguides with separable cross sections, it is also well suited for electromagnetic modeling. Measured and theoretical results for a polarizer with a 90° ± 1° differential phase shift and a return loss better than 35 dB for both polarizations over the operating frequency band confirm the validity of the proposed design.**

***Index Terms*—Mode-matching methods, polarizers, waveguides.**

I. Introduction

Waveguide polarizers are used to convert the polarization of a signal from linear to circular; according to [1] (where the reader is referred for a general discussion on polarization discrimination components), conventional polarizer can be divided into two groups.

The first group comprises devices that convert waves coming from the first interface port with right-hand circular polarization (RHCP) and left-hand circular polarization (LHCP) into the respective linearly polarized dominant modes present at the second interface port, either with square (TE_{10}, TE_{01} modes) or circular cross section (degenerate TE_{11} modes). The final signal separation (e.g., RHCP into TE_{10} and LHCP into TE_{01}) is realized by a sequential ortho-mode transducer (OMT) that supplies the output signals at two separate waveguide ports [2].

The second group is represented by septum polarizers, i.e., devices with three physical interface ports that can be used in order to feed a square (or circular) waveguide radiator in such a way so as to excite either LHCP or RHCP signals [3], [4]. Its input typically consists of two rectangular waveguide ports while its output can take place either in a square waveguide or circular one, the latter solution being commonly adopted for ease of design and manufacturing of circular feeds. Both groups of polarizers, although exhibiting only two and three physical interface ports, electrically represent four-port devices.

Septum polarizers are generally more compact in size since they do not necessitate the presence of an OMT, but they are restricted to operate in the frequency band where only the dominant modes are accessible (i.e., below the TE_{11}/TM_{11} cutoff frequency) because these modes are excited by the unsymmetrical structure and would impair the operation of the device. Roughly speaking, this second group of polarizer presents a narrower bandwidth with respect to the first group. Present increasing demand for wide-bandwidth devices, or possibly with widely separated specific bands (such as satellite bands), makes the first group of polarizer more attractive.

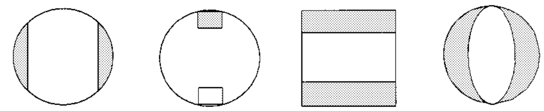

Fig. 1. Type of iris discontinuities used in waveguide polarizer. (a) Classical iris in circular waveguide. (b) Circular ridged waveguide polarizers. (c) Rectangular iris in square waveguide. (d) Proposed elliptical iris in circular waveguide.

These devices have been thus far realized by using either circular or square waveguides with the insertion of various types of iris discontinuity [as illustrated in Fig. 1(a)–(c)]. The use of circular waveguides [5], [6] loaded with irises, such as in Fig. 1(a) and (b), or grooves, such as in [7], causes difficulties from the modeling viewpoint since the irises cross sections are not separable; this fact prevents the application of very efficient modal techniques. On the other hand, square waveguide polarizers [8] with rectangular irises [see Fig. 1(c)] are extremely suitable for electromagnetic-field modeling, but generally require a further transition from square-to-circular waveguide since feeds are generally realized with this latter waveguide.

A possible different solution [9] is to use a supporting waveguide of circular shape loaded with elliptical iris discontinuities, as in Fig. 1(d). The effect of ellipticity on dominant-mode axial ratio was first investigated in [10] and, based on this principle, design and analysis of a squeezed circular waveguide polarizer adjusted by set screws has been presented in [11]. In this paper, we propose a new structure,[1] (see Fig. 2 for a view of the entire polarizer), which combines the advantages of using circular waveguides, the ease of modeling provided by analytically known modal spectra, and complete manufacturing by numerically controlled milling techniques. The polarizer's operating principles, with details on the excited modal patterns at the various iris discontinuities, are discussed in Section II.

It is also noted that very little exists in the literature on the design of iris polarizers, either regarding the initial design or

Manuscript received December 27, 2000.
G. Bertin, B. Piovano, and L. Accatino are with the Telecom Italia Laboratory, 274-10148 Turin, Italy (e-mail: giorgio.bertin@tilab.com; bruno.piovano@TILAB.it; luciano.accatino@tilab.com).

M. Mongiardo is with the Dipartimento di Ingegneria Elettronica e dell' Informazione, Università di Perugia, I-06100 Perugia, Italy (e-mail: Mongiardo@ieee.org).
Publisher Item Identifier S 0018-9480(02)03018-1.

[1] Patent pending.

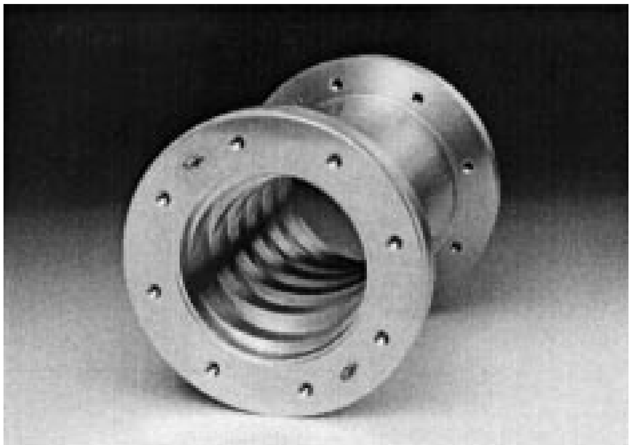

Fig. 2. Polarizer realized in circular waveguide by inserting elliptical waveguide discontinuities.

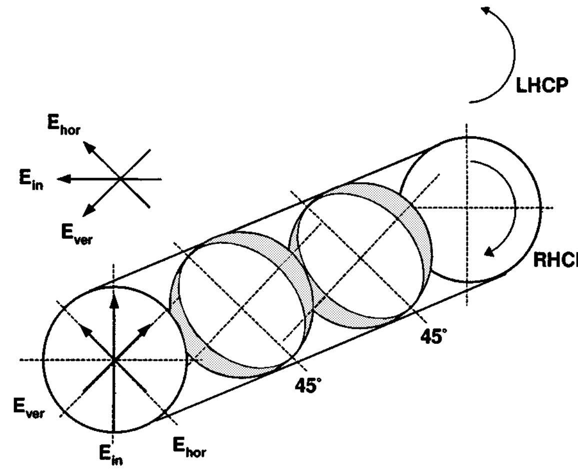

Fig. 3. Polarizer operating principle. A vertical incident field produces a RHCP, while an horizontal incident field produces a LHCP). Note that the irises are inclined of 45°.

the optimization process. Not surprisingly, the optimization part plays a very important role for the successful component design. Unfortunately, an optimization carried out on the entire parameter space (i.e., all geometrical parameters) will almost inevitably lead to local optima solutions, which may be not completely satisfactory in demanding applications. This situation will not be improved by the use of sophisticated optimization techniques, such as space mapping [12], [13] or the adjoint network method [14], [15]; in fact, the problem is not in a lack of efficiency, but rather in the avoidance of local minima.

A hierarchical optimization approach, based on the procedure illustrated in Section III, is proposed here as a viable solution. As a practical illustration, in Section IV, we present theoretical and experimental results for a circular–elliptic polarizer, also considering manufacturability and sensitivity issues.

Finally, of considerable interest is the comparison of the proposed solution with a square waveguide polarizer operating over the same bandwidth. In Section V, we present a discussion of the relevant features of this comparison and, in Section VI, we draw the main conclusions.

II. Polarizer With Elliptical Irises

In Fig. 3, the typical behavior of a waveguide iris polarizer is illustrated. An incident vertical field $\mathbf{E_i}$ may be considered as the superposition of two fields, one with vertical polarization $\mathbf{E_V}$ and one with horizontal polarization $\mathbf{E_H}$. The vertically polarized electric field $\mathbf{E_V}$ propagates along a line loaded by (essentially) capacitive discontinuities, while the field $\mathbf{E_H}$ propagates along a line loaded by (essentially) inductive discontinuities. At the end of the polarizer, after a certain number of irises (in this figure, only two irises are reproduced for clarity), the fields $\mathbf{E_V}$ and $\mathbf{E_H}$ have a phase difference of 90°, hence, producing the sought circular polarization. A RHCP or a LHCP is produced depending on the direction of the incident field, as illustrated in this figure.

Naturally, the polarizer also acts as a polarization discriminator: when an RHCP (LHCP) impinges on the component's right side (Fig. 3), the $\mathbf{E_i}$ linearly polarized field is produced as shown in the figure.

A. Full-Wave Electromagnetic Modeling

Relevant issues in the electromagnetic modeling of discontinuities involving waveguides with elliptical cross sections have been discussed in [16]–[18], and the reader is referred to these papers for a more detailed treatment. In the present context, it is of interest only to provide information on the relevant parameterization pertaining to the particular structure considered.

It is noted that the junction between the circular and elliptical waveguides excites (apart for symmetries) the entire modal spectra. In other words, while in the case of square-to-rectangular waveguides, only TE_{n0} (horizontal step) or LSE^x_{1n} (vertical step) are excited, in the present case, the entire family of modes is excited.

Since the polarizer is symmetrical along the longitudinal (propagation) direction, only 1/2 of the structure needs to be considered. Naturally, in order to compute the differential phase shift between the two polarizations, two different analyses are necessary, one for each polarization. From these two full-wave analyses, we recover the scattering transmission parameters S^H_{21} and S^V_{21}, from which the differential phase $\Delta\Phi$ is computed as $\Delta\Phi = \angle S^H_{21} - \angle S^V_{21}$.

III. Polarizer Optimization

A. General Description of the Hierarchical Optimization Approach

In the hierarchical optimization approach, the overall problem is broken down in a sequence of simpler optimization steps. At the beginning, the designer investigates the most critical aspect to be realized and the associate relevant design parameters, which typically are a subset of the entire parameter space available for the design. Each optimization step is carried out in order to achieve the desired response, but limited to that critical aspect. This procedure is repeated for all the relevant design specifications, hence, smoothly exploring the entire dimensionality of the parameter space while also avoiding several local minima.

B. Application of the Hierarchical Optimization Approach to the Polarizer Design

The polarizer design starts by considering the relevant specifications over the operating bandwidth (f_1–f_2), which, in a typical case are: 1) the differential phase error, with respect to 90° and 2) the return loss lower bound $\mathrm{RL}_{\min}$. It is relevant to observe that an attempt to simultaneously fulfill all the above specifications will generally lead to local minima and poor overall results. Therefore, it is crucial to start by relaxing some of the specifications and to gradually improve the design toward the desired result.

Initially, the focus is on the differential phase requirement, while the return-loss constraint is relaxed (no more than 20 dB). This first part can be considered, and will be denoted in Section III-C, as a differential phase optimization.

Subsequently, we introduce the necessary step transitions between circular waveguides in order to match the feed diameter with that of the polarizer. As an added bonus, in this second optimization part, it is also feasible to optimize for the desired return loss. Hence, this part will be referred to in Section III-D as return-loss optimization.

In Sections III-C and D, we proceed to discuss in more details the differential phase optimization and return loss optimization.

1) Objective Function: The selected objective function is made by the following three different contributions:

1) difference between the actual and specified differential phase at midband;
2) difference of the above quantity as computed at f_1 and f_2;
3) return loss over the operative bandwidth.

Note that 2) essentially enforces a symmetrical differential phase shift over the desired band.

C. Differential Phase Optimization

The differential phase shift is obtained by inserting a certain number of elliptical irises discontinuities. In this case, the relevant parameters for the optimization are as follows:

- polarizer diameter (which, typically, is advantageous to consider different from the feed diameter);
- number of the elliptical iris discontinuities;
- thickness and relative distances of iris discontinuities (the same thickness will be considered for all the irises);
- minor diameter of the elliptical iris discontinuities (while their major diameter will be maintained equal to that of the polarizer envelope).

Since the design is generally carried out from scratch, it is necessary to select the initial values and then run an optimization in order to achieve the desired results. It is recalled that the final objective of this optimization part is to obtain the correct differential phase behavior, in terms of either the operating bandwidth and the desired 90° phase shift. What is not relevant, or only marginally important in this context, is the return-loss requirement.

1) Initial Values: From extensive trials, the following choices of initial values have been selected as appropriate for typical requirements. The polarizer diameter is chosen so as to place the operating band at a roughly equidistant position between the waveguide fundamental-mode cutoff frequency and the frequency of the first higher order mode. A minimal number of 2–3 iris discontinuities is generally necessary as a starting point; this number will be increased later on during optimization upon requirement. The iris thickness (t) and their spacing (s) are selected to be in the range of $\lambda/8 \div \lambda/6$; moreover, at this time, the thicknesses and spacing are assumed to be the same for all irises. Finally, while the major semiaxis of the elliptical iris is maintained equal to the diameter of the polarizer waveguide, the minor semiaxis is chosen to be about 3/4 of the major one.

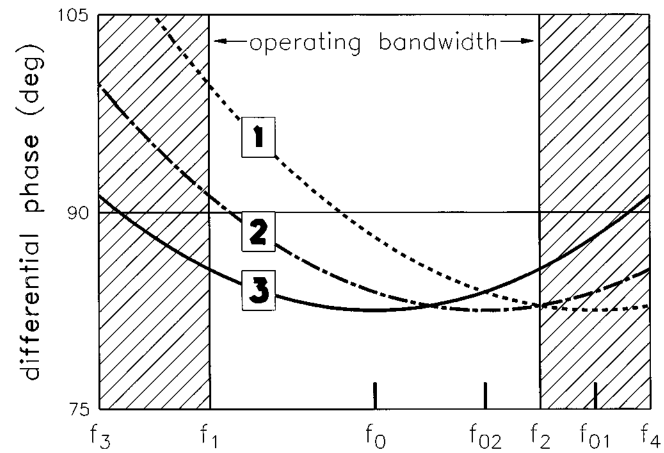

Fig. 4. Frequency-centering procedure: curve 1 = initial, curve 2 = intermediate, curve 3 = final.

2) A Frequency-Centering Optimization: The polarizer frequency response is, at this time, accurately analyzed via a full-wave code; as a result, the differential phase shift is obtained. Generally, the latter has the shape illustrated in Fig. 4, and exhibits a minimum, which is oftentimes out of the desired band of operation. It is, therefore, necessary to carry out a frequency-centering optimization in order to place such a minimum at $(f_1 + f_2)/2$. Four parameters are used for this optimization: the polarizer diameter Φ_{pol}, the spacing s and thickness t of the irises, and the smaller diameter $D_{\min}$ of the elliptical irises. A typical centering procedure can be summarized as follows.

1) The initial analysis of the polarizer over an enlarged bandwidth with respect to the operating frequency band $(f_2 - f_1)$, in order to check the position of the differential phase minimum (see Fig. 4, curve 1); usually this minimum is placed at f_{01}, outside the $f_2 - f_1$ band, e.g., between f_4 and f_2 $(f_4 > f_2)$.
2) A first optimization cycle is carried out over the enlarged $(f_4 - f_1)$ band, imposing a severe constraint on condition 2 of the objective function, but leaving condition 1 relaxed and not considering condition 3; at the end of this optimization cycle, the minimum will be placed at $f_{02} = (f_1 + f_4)/2$, closer to f_0 than f_{01} (see Fig. 4, curve 2).
3) When the minimum falls within the operating band $f_2 - f_1$, a final optimization cycle will shift the minimum exactly to the center $f_0 = (f_1 + f_2)/2$ (see Fig. 4, curve 3).

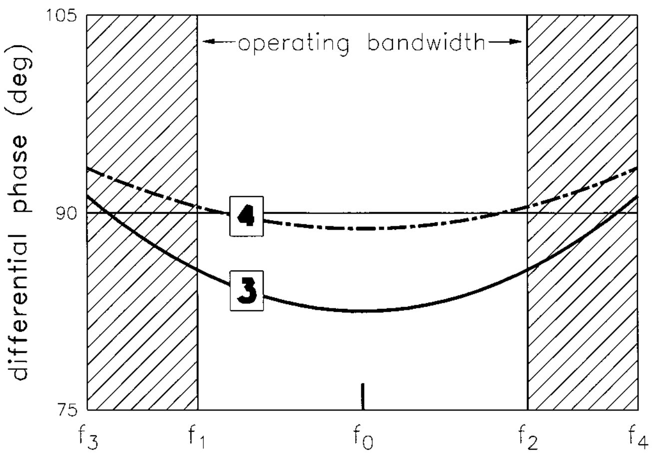

Fig. 5. Reduction of differential phase error in optimization procedure; curve 3 = after frequency centering, curve 4 = after phase error optimization.

4) If the minimum does not fall within the operating band $f_2 - f_1$, the upper optimization frequency f_4 is reduced by an amount equal to $(f_4 - f_2)/n$ with $n = 2, 3, 4, \ldots$; n is the smallest integer value for which the resulting optimization band, narrower than $f_4 - f_1$, but wider than $f_2 - f_1$, includes the minimum; the optimization cycle that follows will move the minimum just to the center of this new optimization band.
5) Point 4) is repeated until the minimum remains within the operating band and the final optimization cycle can start.

After this frequency centering, the minimum of the differential phase curve is moved at the desired position.

3) Reduction of the Differential Phase Error: In order to get the specified value of the differential phase error, it is necessary to increase the number of iris discontinuities used thus far. Naturally, when adding a discontinuity, a further optimization is carried out so as to maintain the minimum at the correct position, while reducing the overall differential error on the operative bandwidth. In this case, the optimization is carried out imposing for the objective function strong constraints on both condition 1 (to minimize the differential phase error) and condition 2 (to maintain the curve symmetry over the operating band), but still leaving condition 3 (return loss) relaxed. The number of irises is iteratively increased until specifications are met (see Fig. 5, curve 4).

D. Return-Loss Optimization

As a result of the previous optimization cycle, a polarizer with the correct differential phase shift has been designed; naturally, the return loss is not yet adequate and the diameter of the polarizer $\Phi_{\rm pol}$ does not match the feed diameter $\Phi_{\rm feed}$. It is, therefore, necessary to add at least two transitions, at both sides of the polarizer, in order to physically connect the latter with the feed. These two transitions are made at the beginning with just two steps; naturally, the diameter of each step transition $\Phi_{\rm step}$ and its length $\ell_{\rm step}$ need to be optimized. The number of steps used for matching and return-loss optimization are then iteratively increased until all specifications are met.

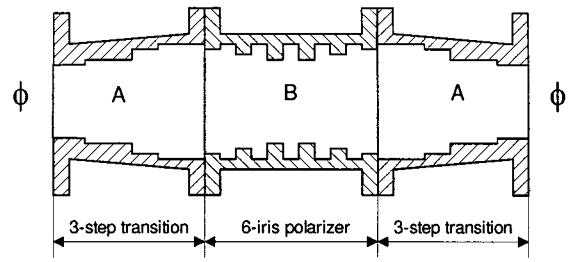

Fig. 6. Schematic view of the realized six-iris circular polarizer (P) along with the circular-to-circular transitions (T).

IV. Circular Waveguide Polarizer—Results

A. Mechanical Realization

The realized component includes inside the polarizer 6 elliptical irises and an input/output three-step circular-to-circular transition (see Fig. 6). The entire component has been realized in aluminum by numerically controlled milling machines with a nominal tolerance of $\pm 10\ \mu$m, which is typically available at specialized workshops. A sensitivity analysis carried out before construction has shown that this tolerance is more than adequate for practical applications at the considered frequency band.

A list of the mechanical geometry follows.

Circular-to-circular transition (T):
- input diameter $\phi = 26$ mm;
- step 1 dia $= 27.44$ mm; length $= 16.65$ mm;
- step 2 dia $= 36.27$ mm; length $= 10.24$ mm;
- step 3 dia $= 40.41$ mm; length $= 16.72$ mm.

Circular polarizer with elliptical irises (P):
- envelope diameter $= 40.41$ mm;
- iris length $= 6.44$ mm (equal for all);
- iris spacing $= 6.12$ mm (uniform);
- iris 1: major axis $= 40.41$ mm; minor $= 36.30$ mm;
- iris 2: major axis $= 40.41$ mm; minor $= 31.46$ mm;
- iris 3: major axis $= 40.41$ mm; minor $= 29.32$ mm.

B. Optimization Cycles and Computer Effort

The number of optimization cycles required to achieve the final design of a polarizer with elliptical irises directly depends on the structure complexity, i.e., on the number of waveguide discontinuities (irises and steps) necessary to meet the electrical requirements (maximum differential phase spreading and input return loss) and on the optimization starting point. The typical number of iterations for a case similar to that shown in Fig. 6 is approximately 1000. The computer effort is obviously related to the number of optimization parameters and that of modes used in the electromagnetic analysis. Still referring to the previous example, the computation time, on an SGI origin 2000 operating at 400 MHz, amounts to be about 4 h with 20 TE input modes and 12 h with 40 TE modes.

C. Comparison Between Measured and Theoretical Results

For verification purposes, before actually manufacturing the component, a further analysis has been carried out with a finite-element code HFSS (High Frequency Structure Simulator, Agilent Technology, Palo Alto, CA, rev. 5.5), with results very

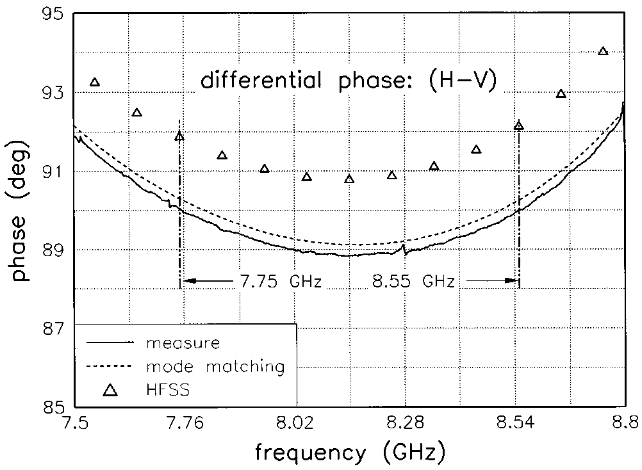

Fig. 7. Elliptical iris polarizer differential phase between vertical and horizontal polarizations. Comparison between theoretical results as obtained by the mode-matching code HFSS and experimental data.

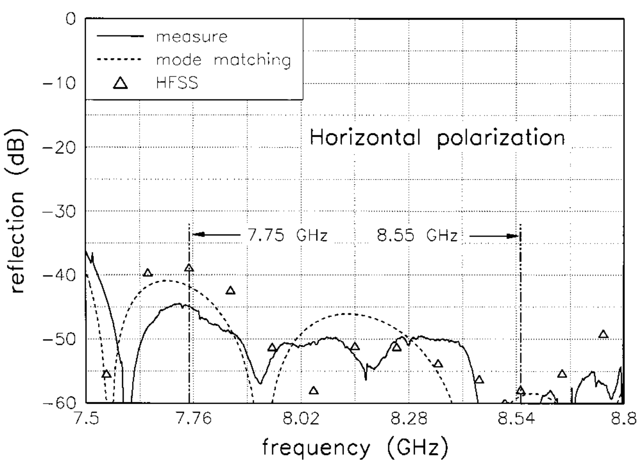

Fig. 8. As in Fig. 7, but for the horizontal polarization return loss.

close to those obtained by modal techniques. The critical parameters to consider for the iris polarizer are the differential phase and the two return losses for the horizontal and vertical polarizations; the relative responses are illustrated in Figs. 7–9, respectively. It is noted a remarkable coincidence of results, i.e., measured and theoretical (both mode matching and HFSS) for what concern the return loss of both polarizations. The measured differential phase is also very close to the mode-matching results, while a modest shift is observed with respect to HFSS.

V. Comparison Between Circular–Elliptic and Square–Rectangular Waveguide Polarizer

Altough square waveguide polarizers are fairly well known [8], little has been published on their manufactured behavior. In [8], a metal-etching manufacturing technique has been proposed, although no measured results have been provided.

During our study and realization of these polarizers, we have found several effects of interest. For reducing manufacturing costs, a clam-shell technology has been considered. It is interesting to note that the clam-shell technology introduces an element of asymmetry for the field present in the waveguides.

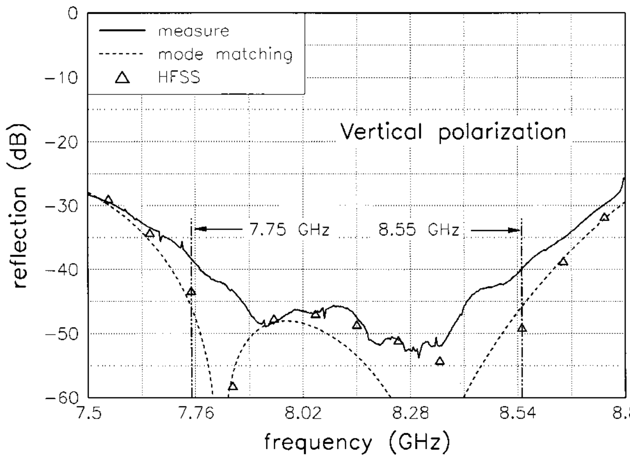

Fig. 9. As in Fig. 8, but for the vertical polarization.

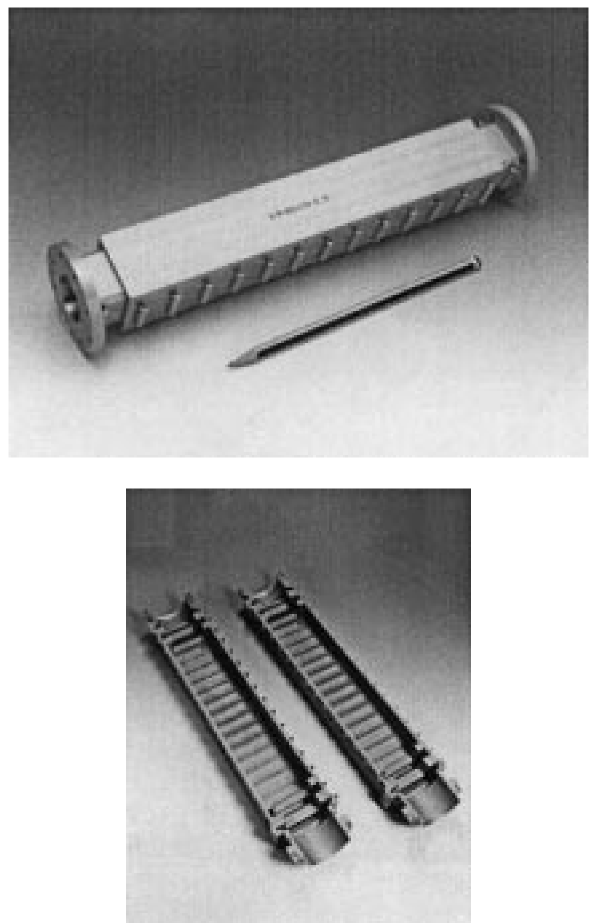

Fig. 10. Clam-shell mounting arrangement of the eight–iris polarizer (top) realized with a square waveguide including two square-to–circular (26-mm diameter) transitions. As an example of clam-shell mounting arrangement (bottom), an open polarizer working in S-band is shown. The clam-shell mounting consists of manufacturing two identical symmetrical halves, which are then joined together.

In fact, with reference to Fig. 10, which represents the used clam-shell mounting arrangement, we have observed two types of phenomena, which we will briefly discuss in Sections V-A and B.

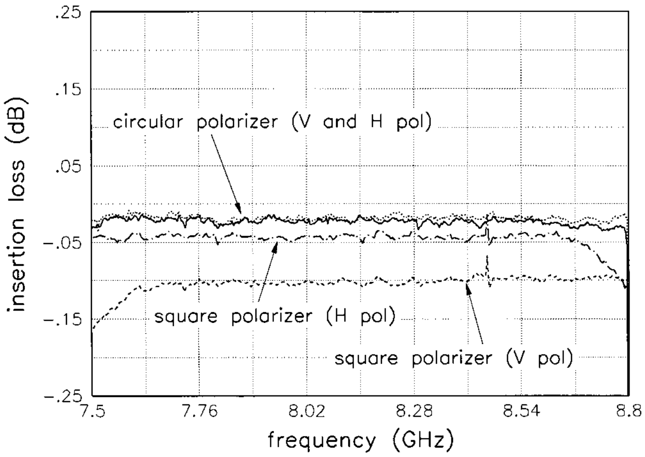

Fig. 11. Measured insertion losses for the square and circular waveguide polarizers. It is apparent that, for the square polarizer, different insertion losses are present on the two polarizations, due to the use of the clam-shell mounting.

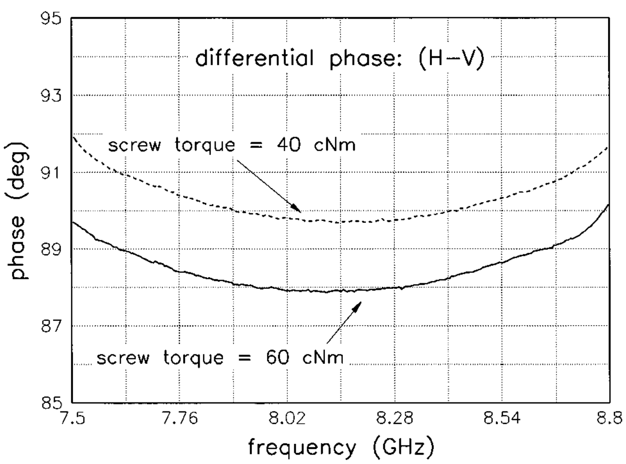

Fig. 12. Measured effect of the mounting screw torque on the realized phase difference.

A. Insertion-Loss Differences for the Two Polarizers

The currents relative to the two field polarizations traveling in the square waveguide are affected in a different manner by the clam-shell arrangement. In particular, for one polarization, the currents flow in the same direction of the waveguide cutting and, therefore, they are modestly perturbed by the latter cutting. On the other hand, for the orthogonal polarization, the waveguide cutting is perpendicular to the currents' flow direction, hence, producing a greater effect.

The above difference has a definite impact on the polarizer performances: in fact, we have observed different insertion losses as represented in Fig. 11. This, in turn, produces a degradation of the circular polarization purity since the two field amplitudes, even if they possess a 90° phase difference, do not have the same amplitude.

From the latter figure, it is also possible to observe that the insertion loss of the circular polarizer is slightly better than that of the square polarizer.

B. Tuning Effects of the Fastening Screws

With reference to the used clam-shell mounting arrangement of Fig. 10, we have also observed that the achieved phase difference realized by the polarizer is dependent on the mounting screw tightness. In Fig. 12, this effect is quantified, showing that a variation of differential phase of about 2° occurs using different values of the screw torque (60 cN · m instead of 40 cN · m). However, while this tuning effect allows the desired phase shift to be achieved, it also introduces a degradation of the design robustness and makes post-production adjustments necessary.

The reason for the mounting screws tuning effects is related to the cross-sectional deformation introduced when tightening the screws. In fact, mechanical deformations introduce a decrease of propagation constant for one polarization, while acting in the opposite way for the orthogonal polarization.

VI. Conclusions

A new design scheme has been presented for iris polarizers in circular waveguides. The differential phase shift between the two orthogonal polarizations is achieved by means of elliptical irises, which are amenable of analytical modal description, hence, allowing the use of accurate and efficient mode-matching codes for the component full-wave analysis.

A hierarchical optimization approach has been introduced as a reliable way for the entire polarizer optimization.

This design permits the use of milling techniques for manufacturing, hence, avoiding more cumbersome approaches as the split-block housing technology. This type of polarizer has been designed, built, and measured, demonstrating the satisfactory agreement between experimental and theoretical results.

The component has been compared with an equivalent polarizer realized with square waveguide and rectangular irises. The square waveguide polarizer has been designed, built, and measured on the same operating bandwidth of the circular polarizer and a comparative discussion of their operating features has been presented.

Acknowledgment

The authors thank the reviewers for their helpful comments and for some valuable references.

References

[1] J. Uher, J. Bornemann, and U. Rosenberg, *Waveguide Components for Antenna Feed Systems: Theory and CAD*. Norwood, MA: Artech House, 1993.

[2] M. Ludovico, G. Zarba, B. Piovano, G. Bertin, L. Accatino, and M. Mongiardo, "CAD and optimization of compact ortho-mode transducers," *IEEE Trans. Microwave Theory Tech.*, vol. 47, pp. 2479–2486, Dec. 1999.

[3] R. Behe and P. Brachat, "Compact duplexer–polarizer with semicircular waveguide," *IEEE Trans. Antennas Propagat.*, vol. 39, pp. 1222–1224, Aug. 1991.

[4] B. Piovano, G. Bertin, L. Accatino, and M. Mongiardo, "CAD and optimization of compact wide-band septum polarizers," presented at the Eur. Microwave Conf., Munich, Germany, 1999.

[5] J. Bornemann, S. Amari, J. Uher, and R. Vahldieck, "Analysis and design of circular ridged waveguide components," *IEEE Trans. Microwave Theory Tech.*, vol. 47, pp. 330–335, Mar. 1999.

[6] J. Pyle, "Circular polarizers of fixed bandwidth," *IEEE Trans. Microwave Theory Tech.*, vol. MTT-12, pp. 557–559, Sept. 1964.

[7] N. Yoneda, M. Miyazaki, H. Matsumura, and M. Yamato, “A design of novel grooved circular waveguide polarizers,” *IEEE Trans. Microwave Theory Tech.*, vol. 48, pp. 2446–2452, Dec. 2000.

[8] U. Tucholke, F. Arndt, and T. Wriedt, “Field theory design of square waveguide iris polarizers,” *IEEE Trans. Microwave Theory Tech.*, vol. MTT-34, pp. 156–160, Jan. 1986.

[9] G. Bertin, B. Piovano, L. Accatino, and M. Mongiardo, “Analysis and design of circular waveguide polarizers with elliptical irises,” in European Microwave Conference, Paris, 2000.

[10] P. I. Sandsmark, “Effect of ellipticity on dominant-mode axial ratio in nominally circular waveguides,” *IRE Trans. Microwave Theory Tech.*, vol. MTT-3, pp. 15–20, Oct. 1955.

[11] K. Sarabandi, “A waveguide polarization controller,” *IEEE Trans. Microwave Theory Tech.*, vol. 42, pp. 2171–2174, Nov. 1994.

[12] J. Bandler, R. Biernacki, and S. Chen, “Fully automated space mapping optimization of 3D structures,” in *IEEE MTT-S Int. Microwave Symp. Dig.*, June 1996, pp. 753–756.

[13] J. Bandler, R. Biernacki, S. Chen, and D. Omeragic, “Space mapping optimization of waveguide filters using finite element and mode-matching electromagnetic simulators,” in *IEEE MTT-S Int. Microwave Symp. Dig.*, vol. 2, June 1997, pp. 635–638.

[14] F. Alessandri, M. Mongiardo, and R. Sorrentino, “New efficient full wave optimization of microwave circuits by the adjoint network method,” *IEEE Microwave Guided Wave Lett.*, vol. 3, pp. 414–416, Nov. 1993.

[15] M. Mongiardo and R. Ravanelli, “Automated design of corrugated feeds by the adjoint network method,” IEEE Trans. Microwave Theory Tech., vol. 45, pp. 787–793, May 1997.

[16] P. Matras, R. Bunger, and F. Arndt, “Modal scattering matrix of the general step discontinuity in elliptical waveguides,” *IEEE Trans. Microwave Theory Tech.*, vol. 45, pp. 453–458, Mar. 1997.

[17] L. Accatino, G. Bertin, and M. Mongiardo, “Elliptical cavity resonators for dual-mode narrowband filters,” *IEEE Trans. Microwave Theory Tech.*, vol. 45, pp. 2393–2401, Dec. 1997.

[18] M. Mongiardo and C. Tomassoni, “Modal analysis of discontinuities between elliptical waveguides,” *IEEE Trans. Microwave Theory Tech.*, vol. 48, pp. 597–605, Apr. 2000.

Giorgio Bertin (M’92) was born in Aosta, Italy, in 1956. He received the Doctor degree in electronic engineering from the Polytechnic School of Turin, Turin, Italy, in 1982.

In 1983, he joined the Microwave Department, Centro Studi e Laboratori Telecomunicazioni S.p.A. (CSELT) (now the Telecom Italia Laboratory), Turin, Italy, where he was initially engaged in dielectric oscillator and dielectric-loaded cavity design. His activities then focused on the modeling of microwave discontinuities and the computer-aided design of guiding structures, with particular attention devoted to discontinuities between nonstandard waveguides, such as those involving a dielectric loading or the presence of ridges. He currently supervises all activities related to electromagnetic modeling in the Microwave Department.

Bruno Piovano (A’92) was born in Turin, Italy, in 1953. He received the Doctor degree in electronic engineering from the Polytechnic School of Turin, Turin, Italy, in 1978.

In 1980, he joined the Microwave Department, Centro Studi e Laboratori Telecomunicazioni S.p.A. (CSELT) (now the Telecom Italia Laboratory), Turin, Italy. He initially developed a basic and comprehensive software package for analyzing complex beam-forming networks accounting for the electromagnetic model of subcomponents. He then became a Senior Researcher responsible for the design of waveguide networks in the INTEL-717 “exible/reconfigurable antenna” study and in the European Space Agency “Butler matrix amplifier” and “contoured beam reconfigurable antenna” studies. His current activities regard the design of high-performance waveguide subsystems, with particular attention to antenna feed networks.

Luciano Accatino (M’84) was born in Turin, Italy, in 1950. He received the Doctor degree in electronic engineering from the Polytechnic School of Turin, Turin, Italy, in 1973.

In 1975, he joined the Centro Studi e Laboratori Telecomunicazioni S.p.A. (CSELT) (now the Telecom Italia Laboratory), Turin, Italy, where he was initially engaged in the design of microstrip circuits and components. In 1980, he became involved in the design and development of microwave cavity filters and, subsequently, of various components for beam-forming networks. He then supervised the activities related to filters and waveguide components at CSELT, stimulating a wide application of electromagnetic models to the design of all passive components. Since 1994, he has been the Head of the Microwave Department.

Mauro Mongiardo (M’91–SM’00) received the Laurea degree (*summa cum laude*) from the University of Rome, Rome, Italy, in 1983, and the Ph.D. degree from the University of Bath, Bath, U.K., in 1991.

He is currently an Associate Professor at the Università di Perugia, Perugia, Italy. He was a Visiting Scientist at the University of Victoria, Victoria, BC, Canada, the University of Bath, Bath, U.K., Oregon State University, Corvallis, and the Technical University of Munich, Munich, Germany. His main contributions are in the area of modeling of waveguide discontinuities, both in the cases of closed waveguides and open waveguides such as microstrip lines or coplanar waveguides. His research interests include numerical methods with contributions in the areas of mode-matching techniques, integral equations, variational techniques, finite difference time domain (FDTD), transmission line matrix (TLM), and finite-element method (FEM). He is also involved with frequency- and time-domain analysis of monolithic microwave integrated circuits (MMICs) and is currently interested in the modeling and computer-aided procedures for the design of microwave and millimeter-wave components.